



Cite this: *Environ. Sci.: Adv.*, 2025, 4, 77

## Hydroxyapatite/urea hybrid materials: what is the basis for the enhanced nutrient efficiency?

Mohamed Ammar,<sup>a</sup> Sherif Ashraf<sup>b</sup> and Jonas Baltrusaitis \*<sup>a</sup>

The growing demand for food production worldwide has led to the increased use of fertilizers contributing to a range of environmental problems. To reduce these problems, the development of urea–hydroxyapatite (HAP) materials as nutrient-efficient fertilizer carriers has gained considerable attention as a more nutrient-efficient alternative to conventional nitrogen (N) and phosphorus (P) fertilizers. Conventional N fertilizers, such as urea, possess high solubility and rapidly release nitrogen leading to significant nutrient losses through leaching and volatilization. Conventional P fertilizers suffer from quite the opposite problem: they are quickly immobilized in soil and P release becomes very slow. HAP is a naturally occurring mineral and has been postulated, at the nanoscale, to release P at a controlled rate although risks associated with HAP nanoparticle occupational and environmental toxicity remain. HAP/urea hybrid materials present a unique opportunity for N–P–(Ca) fertilizer material design where innate properties of the parent materials, urea and HAP, are altered due to the purported chemical interactions, thus resulting in a novel and improved nutrient management paradigm. This review summarizes the developments in their synthesis, nutrient release and plant uptake while scrutinizing the reported underlying chemical interactions between both parent compounds, critical to the enhanced efficiency in soil.

Received 12th June 2024  
Accepted 20th October 2024

DOI: 10.1039/d4va00197d

rsc.li/esadvances

### Environmental significance

Phosphorus (P) and nitrogen (N) are essential nutrients for all life forms but have turned into major contaminants. For instance, excessive application of P as an agricultural fertilizer has resulted in the leaching of P out of soil and caused eutrophication of water bodies and compromised the quality of drinking water. Similarly, excessive use of urea as a N fertilizer resulted in reactive nitrogen mobilization into the environment. Nevertheless, these major nutrients are critical for the growth of crops, as well as the functioning of aquatic/terrestrial organisms. The balanced release of nutrients into soil is hence of major importance. This review describes the development and open question in structure–property relationships of urea–hydroxyapatite materials recently proposed as nutrient-efficient fertilizers.

## 1. Introduction

By the year 2050, the world's population is projected to reach ten billion<sup>1,2</sup> posing a significant challenge in providing adequate food supply to meet the growing demand.<sup>3</sup> To address this challenge, synthetic nitrogen (N) fertilizers play a crucial role, as they account for half of the global food production.<sup>4</sup> Nitrogen is a vital nutrient essential for life and food production.<sup>5</sup> Only about half of the applied nitrogen is taken up and the excess is either temporarily stored in soil or lost to the environment.<sup>4</sup> Nitrogen losses can lead to nitrogen pollution, which is a significant concern with far-reaching environmental impacts.<sup>5,6</sup> These impacts include eutrophication, air pollution, biodiversity loss, climate change, and stratospheric ozone depletion.<sup>7,8</sup> These detrimental effects of excessive nitrogen

inputs are already evident causing a decline in herbaceous plant species richness in terrestrial and wetland ecosystems worldwide. Additionally, nitrogen pollution can have adverse effects on human health, contributing to respiratory ailments, cardiac diseases, and various cancers.<sup>7,9,10</sup> To reduce the environmental problems associated with nitrogen pollution, global efforts are essential<sup>11</sup> and developing methods and formulations of more sustainable N fertilizer materials can be the key to the solution.

In addition to the concerns related to nitrogen pollution, there are also issues with phosphorus (P) fertilizers from environmental and economic aspects.<sup>12</sup> The global demand for P fertilizers has been on the rise leading to intensified mining and production activities. However, this surge in P utilization has come at a steep environmental cost.<sup>12</sup> One of the key environmental concerns associated with phosphorus fertilizers is the resulting eutrophication.<sup>12,13</sup> P runoff from agricultural fields often finds its way into water bodies promoting excessive algal growth. As a result, water bodies become overloaded with nutrients, leading to harmful algal blooms and the formation of “dead zones” where oxygen levels become dangerously low and

<sup>a</sup>Department of Chemical and Biomolecular Engineering, Lehigh University, 111 Research Dr, Bethlehem, PA 18015, USA. E-mail: job314@lehigh.edu; Tel: +1-610-658-6836

<sup>b</sup>Department of Physics, Faculty of Science, Suez University, Suez 43518, Egypt



threaten aquatic life.<sup>14,15</sup> In addition to eutrophication, P mining and fertilizer production generate substantial processing waste, such as phosphogypsum, which contains toxic elements, such as cadmium and radioactive substances.<sup>16,17</sup> Altogether, there is a pressing need to improve P and N management practices and adopt novel more efficient fertilizers to minimize nutrient losses and their adverse environmental impacts.

The compound of urea and hydroxyapatite (HAP) in an integral hybrid material can potentially offer significant advantages over the conventional mixture of these fertilizers.<sup>18</sup> The tunable nutrient release properties of HAP nanoparticles can ensure a controlled and sustained release of phosphorus, reducing the risk of nutrient leaching and runoff into water bodies.<sup>19</sup> Additionally, the controlled release of urea can potentially take place if it undergoes specific binding interaction with HAP which can enhance nitrogen efficiency, ensuring that nitrogen is readily available to plants during critical growth stages while minimizing nitrogen losses as greenhouse gas emissions.<sup>18</sup> Consequently, the use of HAP/urea hybrid materials can significantly reduce the environmental footprint of agricultural practices contributing to the overall reduction of greenhouse gas emissions and improved air quality. This work reviews the body of reported literature data where a hybrid HAP/urea material was synthesized and used in agricultural experiments as a compound N-P-(Ca) fertilizer. The measured and observed improvements in nutrient release are first described while scrutinizing the potential underlying molecular interaction phenomena responsible for the improvement of nutrient release.

## 2. HAP as an emerging P fertilizer material

HAP holds promise as a highly efficient P fertilizer in modern agriculture. One of its remarkable characteristics is the naturally rich composition of essential macronutrients, including calcium (Ca) and P, which are crucial for plant growth and development. These nutrients are readily available within apatite ensuring a readily accessible and valuable nutrient source for plants thus promoting healthy growth and higher yields.<sup>20,21</sup> Furthermore, HAP's biocompatible nature, in general, makes it an environmentally friendly option for agricultural use.<sup>22,23</sup> This biocompatibility enhances its potential for sustainable and eco-friendly farming practices. The particle size of HAP plays a significant role in enhancing its performance as a fertilizer if it obtains a large surface-to-volume ratio.<sup>24,25</sup> While outside the scope of this review, the particle size of HAP has also been shown to be important due to the potential toxicity and needs to be accurately addressed<sup>26</sup> before a wide-ranging application is permitted.

Furthermore, the pH-responsive solubility of HAP is a standout feature that sets it apart from conventional P fertilizers.<sup>27,28</sup> This property allows HAP to respond dynamically to changes in soil pH levels, releasing calcium and phosphate ions only when needed by the plants. This targeted and gradual nutrient release aligns with crop growth stages, avoiding nutrient wastage and leaching. As a result, the enhanced



Fig. 1 HAP/urea hybrid materials are proposed to achieve equivalent NUE compared to conventional fertilizers but at a lower application rate. Therefore, the recommended doses in the conventional N-fertilizers can be scaled to reach the same NUE.

nutrient uptake efficiency promotes crop health and resilience, contributing to improved agricultural sustainability. Sajadina *et al.* investigated the effects of four different types of fertilizers on the growth properties of *Zea mays* L. Among them, HAP fertilizers demonstrated the most significant impact on maize growth. In comparison to conventional commercial fertilizers, such as simple and triple superphosphate (SSP and TSP), HAP-based fertilizers exhibited higher effectiveness in improving maize traits. HAP increased the height of maize by 50% more than SSP and control, in addition to 36% compared to TSP.<sup>25</sup>

Finally, HAP offers an expansive surface area for interactions with other nutrient-containing compounds.<sup>24</sup> This property enables efficient adsorption of essential elements onto its surface, promoting controlled nutrient release and uptake by plants over time.<sup>29</sup> Another advantage of HAP lies in its adaptability to cation or anion doping, providing a versatile platform for tailoring its properties to specific agricultural needs.<sup>30-32</sup> This flexibility enables researchers to design the characteristics of fertilizer based on HAP, including nutrient release rates and compatibility with different soil types and crops, for optimized agronomic outcomes. One such quickly developing area is the design of N-P-(Ca) fertilizer materials where HAP is used to stabilize urea and decrease nitrogen release rates. As shown in Fig. 1, the goal of such a design must include significantly improved nitrogen management that decreases the need for high-applied nutrient loading to achieve the same nitrogen utilization efficiencies (NUEs).

## 3. Preparation of HAP and HAP/urea

HAP used in HAP/urea hybrid materials can be synthesized using several methods but mainly there are six methods for the preparation. These methods are summarized in Fig. 2 and the most used method in preparing composites of HAP/urea is the wet method. Tarafder *et al.* used the wet method by reacting solutions of calcium hydroxide and orthophosphoric acid to obtain precipitated HAP.<sup>33</sup> They also modified urea by adding trisodium citrate to work as a nitrification inhibitor and heated the mixture to 90 °C for 1 h. The preparation of HAP/urea involved mixing 100 mL of HAP suspension with 0.05 g of synthesized urea. The dispersion was sonicated at 30 kHz for 1 hour, followed by





Fig. 2 The common methods of HAP preparation with their related techniques. HAP/urea is typically synthesized by the wet method which is highlighted with a green color and the effect of other synthesis methods on the resulting structure-nutrient release properties is largely unknown.

settling and removal of excess liquid. The resulting mixture was then centrifuged and washed. The resulting composite was dried at 100 °C for 2 hours and powdered using a hand mortar.<sup>33</sup> The same method was used by Kottegoda *et al.* by dissolving 75 kg of solid urea in a 75 L suspension of Ca(OH)<sub>2</sub> (9.65 kg). The mixture was stirred for 45 minutes before adding 5.05 L of 0.6 M H<sub>3</sub>PO<sub>4</sub> dropwise. The resulting composite had a urea : HAP ratio of 6 : 1 and was mechanically agitated for an additional 2 h. Finally, the mixture dispersion was flash-dried at 60 °C to obtain the HAP/urea material.<sup>34</sup> Another study by Fernando *et al.* reported fabrication of HAP on quartz crystal microbalances (QCMs) by depositing HAP particles with rod-like and bead-like morphologies onto 10 MHz QCM crystals with 100 nm-thick gold electrodes. The HAP particles were synthesized *via* two routes (R1 and R2) and deposited using spin coating and electrophoretic deposition (EPD) techniques to achieve (100) and (002) preferential crystal orientations. 1-hour ultrasonic dispersion of HA-Np powder in absolute ethanol was used to prepare the HAP suspension. Spin coating was performed at 3500 rpm for 5 minutes using HAP synthesized *via* R1, while EPD was carried out

at 10 V for 6 seconds using HAP prepared *via* R2. The coatings were then treated with ultrasonic waves (28 kHz, 100 W) for 5 seconds to remove loosely bound particles and heat-treated for 3 h using a tungsten lamp.<sup>35</sup> The reported methods by Ullah *et al.*, Maghsoodi *et al.* and Madusanka *et al.* were the same methods and steps as those by Kottegoda *et al.* with a ratio of 1 : 1 for urea : HAP in Madusanka's and 7 : 1 in Maghsoodi's work.<sup>36–38</sup>

#### 4. HAP/urea hybrid materials for enhanced plant nutrient uptake – equilibrium considerations

As further scrutinized in Section 5, urea molecules can bind to the HAP particle surface potentially leading to a lower N solubility although the exact binding or slower N release mechanism for this is unclear. Kottegoda *et al.* synthesized HAP/urea with a weight ratio of 6 : 1. They showed that equivalent N amount release took 12 times longer for HAP/urea than for pure urea in column dissolution experiments. Moreover, HAP/urea was associated with improved rice crop yields at a 50% lower applied nitrogen content. It was proposed due to the interaction of urea and HAP *via* amine and carbonyl groups.<sup>34</sup> Similarly, Pohshna *et al.* synthesized HAP/urea materials with a 5 : 1 weight ratio deemed as urea-doped HAP nanomaterials although experimental procedures were sol–gel at low temperatures, unlikely to result in doping. Application of these materials in rice fertilization with N<sub>60</sub> : P<sub>175</sub> : K<sub>50</sub>, a half-recommended dose of N<sub>120</sub> : P<sub>60</sub> : K<sub>50</sub>, resulted in comparable biomass yields and plant height, as compiled in Table 1.<sup>39</sup> The results also depicted a high efficacy of N use (76%) and P (14%), which revealed a significant reduction in nutrient leaching.<sup>39</sup> While non-comprehensive, their results provide the potential of hybrid HAP/urea materials to yield biomass growth performance indicators while using half of the nitrogen in standalone urea.

Carmona *et al.* reported that the cost per gram for amorphous calcium phosphate/urea (ACP) is relatively higher than that of the known market fertilizers such as diammonium and monoammonium phosphates. The reported prices were 0.08€ per g for ACP/urea, while 0.038 and 0.032€ per g for diammonium and monoammonium phosphates respectively.<sup>40</sup>

Table 1 Comparison of the growth efficiency of HAP/urea hybrids with conventional fertilizers. The plant growth in control samples was normalized to 100%

Treatment	Plant	Biomass weight (%)	Plant height (%)	Yield (%)	Ref.
HAP/urea N <sub>120</sub> kg of nitrogen per ha : P <sub>350</sub> : K <sub>50</sub> (recommended dose)	Rice	129	115	—	39
HAP/urea N <sub>60</sub> : P <sub>175</sub> : K <sub>50</sub> (half of the recommended dose)		124	113	—	
N <sub>120</sub> : P <sub>60</sub> : K <sub>50</sub>		125	108	—	
N <sub>0</sub> : P <sub>0</sub> : K <sub>0</sub> (control)		100	100	—	
Urea <sub>100</sub> kg ha <sup>-1</sup>	Rice	—	—	131	34
HAP/urea <sub>50</sub> kg ha <sup>-1</sup>		—	—	142	
N <sub>0</sub> : P <sub>0</sub> : K <sub>0</sub> (control)		—	—	100	



Furthermore, 2.5 and 3.7€ are needed to obtain 1 mol of N in diammonium and monoammonium phosphates, respectively, while 17.3€ per mol per N for ACP/urea. Therefore, it can be seen that HAP/urea can potentially provide higher efficiency and sustainability but at a higher price.

## 5. Release rates of nitrogen from HAP/urea hybrids – kinetic considerations

The use of HAP as a stabilizing agent to mitigate nitrogen release presents an intriguing concept. Recent studies have demonstrated the remarkable ability of HAP nanorods to reduce the release rate of complexed urea by up to 11.5 times when compared to pure urea.<sup>38</sup> They reported that pure urea completely dissolved in deionized water after 40 seconds while HAP/urea reached around 90% of urea release after 480 seconds.<sup>38</sup> Kottegoda *et al.* also found that HAP/urea had a slower rate of N release than pure urea more than 12 times, which is similar to the work reported by Maghsoodi *et al.*<sup>34,38</sup> In particular, in these experiments, around 99% of N in urea was released after 320 seconds while in HAP/urea (1 : 6) around 86% was released in water after 3820 seconds and the rest 14% was released after a week as shown in Table 2.<sup>34</sup> Tarafder *et al.* showed that HAP/urea exhibited a slow release rate of nutrients in soil as well as water although the underlying reasons why the nutrient release in water is much slower than in soil were not obvious. After 14 days, around 0.1% and 1% of  $\text{NO}_2^-$  was released in water and soil, respectively, from urea-modified HAP particles. In addition,  $\text{PO}_4^{3-}$  released after 14 days was 1% and 6% in soil and water, respectively.<sup>33</sup> Interestingly, the authors observed ~320%  $\text{NO}_3^-$  release in the soil after 14 days but did not elaborate on this apparent nitrogen balance increase. Finally, Madusanka *et al.* showed that the HAP/urea/montmorillonite composite exhibited N release patterns that were much slower than those in pure urea. In particular, in the soil column, urea released around 70% of N after 30 days while HAP/urea/montmorillonite reached the same released amount 20 days later.<sup>37</sup> Hence, kinetic release patterns of hybrid HAP/urea materials are reported to be different from those of pure urea and nutrient release patterns reported so far paint a complex picture with implications of strongly inhibited urea dissolution from HAP/urea materials.

## 6. Interactions between HAP and urea potentially responsible for the improved N stability

### 6.1. Structural interactions between HAP and urea

The crystal structure investigation has a pivotal role in its capacity to improve the understanding of the interactions between urea and HAP. Interactions between different materials hold the potential to induce vacancies, structural imperfections, and even distortion. Hence, through the identification of plane shifts or alterations in intensity, the governing interactions that drive these changes can be indicated. Pure urea exhibits distinct peaks at 22.25°, 29.32°, 24.62°, 35.53°, and 37.12°, corresponding to Miller indices of (110), (111), (101), (210), and (201), respectively.<sup>41</sup> Notably, the most pronounced peak corresponds to the (110) plane. On the other hand, HAP shows two main types of crystal structures which are hexagonal and monoclinic. The most used one in agricultural applications is the hexagonal crystal symmetry. The hexagonal symmetry belongs to the  $P6_3/m$  space group and a hexagonal unit cell. The crystallographic parameters of  $a$  and  $c$  are 9.418 and 6.881 Å, respectively.<sup>42</sup>

HAP within the compound material with urea can be obtained with various crystallinities from amorphous to the highly crystalline bulk. This depends primarily on the synthesis method conditions. Elhassani *et al.* prepared HAP by a chemical approach and then a well-dispersed solution was obtained for both urea and HAP. The XRD analysis showed the hexagonal symmetry of HAP. The existence of urea was detected using its tetragonal symmetry and, after washing, the urea was still detected by XRD. This indicated the strong bonding between urea and HAP within the hybrid material. This impregnation technique of urea addition led to no change or modification in the HAP structure.<sup>43</sup> In a study by Sharma *et al.*, urea exhibited prominent peaks for ( $hkl$ ) planes of (210), (111), and (110). These planes showed shifts due to the structural modifications and rearrangements.<sup>31</sup> Some peaks disappeared such as the peak belonging to the (110) plane. Therefore, the incorporation of urea on the HAP surface can lead to a change in the urea structure. The difference between the preparation in Elhassani's and Sharma's work was the temperature of the preparation. Sharma *et al.* used 50 °C during HAP preparation and mixing with urea. However, Abeywardana *et al.* synthesized HAP/urea

Table 2 Release behavior of traditional and slow-release compounds of HAP/urea

Fertilizer type	Release pattern	Conditions	Authors	Ref.
Traditional urea	100% release in 40 seconds	In water	Maghsoodi <i>et al.</i>	38
	99% release in 320 seconds	In water	Kottegoda <i>et al.</i>	34
	70% release in 30 days	In soil	Madusanka <i>et al.</i>	37
HAP/urea hybrids	90% release in 480 seconds	In water	Maghsoodi <i>et al.</i>	38
	86% release in 3820 seconds	In water	Kottegoda <i>et al.</i>	34
	The remaining 14% were released over 7 days	In water	Kottegoda <i>et al.</i>	34
	70% release in 50 days	In soil	Madusanka <i>et al.</i>	37
	0.1% $\text{NO}_2^-$ and 1% $\text{PO}_4^{3-}$ release in 14 days	In soil	Tarafder <i>et al.</i>	33
	1% $\text{NO}_2^-$ and 6% $\text{PO}_4^{3-}$ release in 14 days	In water	Tarafder <i>et al.</i>	33



Table 3 The various compositions and their detection using XRD

Composition	Crystal size (nm)	Crystalline information	Results	Ref.
HAP (control)	27	—	100% (plant height)	44
Zn-HAP/urea	—	Peaks of HAP have no shifts	133% (increased plant height)	
Cu-Fe-Zn-HAP/urea	—	Significant breakdown in the peak at 22.1° of the urea crystal structure	Statistically significant nutrient uptake efficiency of <i>A. esculentus</i> at 50 mg per week	33
Urea-coated HAP nanorods	18	There was no shift in HAP or the urea structure. But the plane of (210) of urea has decreased in intensity after coating	50% urea reached the same results as those of 50% urea in HAP/urea	34
HAP	38.7	—	—	31
HAP/urea	—	There was a shift in urea peaks in planes (210) and (111) compared to pure urea	50% and even 25% of N doses in the doped-HAP/urea hybrid can obtain results similar to those of 100% N doses of conventional urea	
Zn-HAP/urea	28.3			
Mg-HAP/urea	20.8			

composites and observed no peak shifts in HAP (hexagonal structure) upon the incorporation of urea.<sup>44</sup> There was no elevation in temperature during the preparation. Hence, this might indicate that higher temperatures during the mixing step of urea and HAP can lead to structural modifications in urea.

Other nutrients were also incorporated into HAP/urea hybrid materials. Zn-HAP/urea composites resulted in higher plant height and dry weight, as shown in Table 3. Tarafder *et al.* demonstrated that urea exhibited lower intensity peaks, indicating possible disruption of the crystal structure due to interaction with HAP.<sup>33</sup> They attributed this effect to a metal-ligand interaction between N and Ca atoms in newly formed HAP/urea composites. They also showed that when *A. esculentus* plants were treated with a low weekly dose (50 mg) of Cu-Fe-Zn-HAP/urea fertilizer they exhibited a statistically significant increase in nitrogen utilization efficiency. Interestingly, G. Ramírez-Rodríguez *et al.* observed that the intense peak of urea at 22° upon its incorporation into amorphous calcium phosphate – but only at the amounts below those leading to phase segregation – transformed completely into an amorphous pattern with a broad amorphous peak at 32.5°.<sup>45</sup> This means that the incorporation of urea into the hybrid HAP/urea material can indeed be a single phase, as long as the concentrations allow excess urea leading to phase segregation. For this reason, some high urea content HAP/urea composites exhibited crystalline patterns of the segregated parent compounds.<sup>34</sup> Sharma *et al.* studied the effect of Zn/Mg doped HAP/urea on wheat growth usage.<sup>31</sup> The results showed that elemental dopants can be used to manipulate the crystallinity of HAP and thus the nitrogen loading capacity.<sup>31</sup> In addition, using 50% and 25% of Zn/Mg-HAP/urea promoted wheat growth similar to the 100% doses of urea.<sup>31</sup> Noteworthy, HAP or HAP/urea hybrids did not exhibit a typical crystalline pattern of HAP observed making peak shifts of urea in the HAP structure upon doping Mg and Zn difficult to be assigned.

It can be seen in Table 3 that the incorporation of urea did not significantly affect the crystallite size of prepared HAP, as determined from XRD analysis. Crystallite size can be used as an important indicator if the crystallinity of the material is

changing due to the urea incorporation into the HAP structure (or *vice versa*) but the concentrations of the parent materials, and likely synthesis methods, need to be adjusted to achieve it.

## 6.2. Chemical interactions between HAP and urea

The impact of the interaction between HAP and urea can crucially affect the urea reactivity and N release properties. The reported molecular binding mechanisms are described in this section.

Ullah *et al.* prepared HAP/urea hybrid materials and detected C–N, C=O, and N–H vibrations and the presence of the PO<sub>4</sub><sup>3–</sup> functional groups in the final composite material.<sup>36</sup> The peak at 1643 cm<sup>–1</sup> was assigned to the C=O functional group. However, ν(CO) in urea is typically found at 1601 cm<sup>–1</sup> and the combination of peaks in the 1700–1400 cm<sup>–1</sup> spectral region is due to the combination of bending and stretching modes of –NH<sub>2</sub> and –CN functional groups with some combinations of ν(CO).<sup>46</sup> The peak at 1640 cm<sup>–1</sup> can often be due to the presence of adsorbed water vibrations.<sup>47</sup> In this situation, a series of samples synthesized with increasing urea content would allow for unambiguous infrared peak assignments.

Kottegoda *et al.* presented X-ray photoelectron spectroscopy (XPS) spectra where the N 1s peak of HAP nanoparticles exhibited a peak at 399.2 eV while the HAP/urea hybrid material exhibited a peak shifted to 400.7 eV. Therefore, new bonds were proposed to have formed between HAP and N of urea. Furthermore, Ca 2p, and P 2p of HAP/urea showed higher binding energy than pure HAP by 0.3 eV. The author attributed the shift in peak binding energy to changes in the chemical environment around Ca<sup>2+</sup> ions and H-bonding formation between PO<sub>4</sub><sup>3–</sup> groups and urea.<sup>34</sup> They correlated these observations with the FTIR results where a shift in C=O and N–C–N towards lower wavenumbers was observed, as shown in Fig. 3. In addition, the intensity of NH<sub>2</sub> decreased when urea and HAP were in one composite which indicates that fewer molecules are vibrating at certain frequencies. Therefore, fewer bonds are formed at these specific frequencies. This might indicate destruction in the urea structure. However, chemically pure HAP alone should not contain any nitrogen atoms. XPS



analysis presented by Kottegoda *et al.*<sup>34</sup> is somewhat misleading since Fig. 3 in that reference refers to N 2s but the region presented is N 1s. It can only be surmised that HAP nanoparticles were contaminated or made using a different method that included an external nitrogen source, for example,  $\text{NH}_4\text{OH}$  for pH adjustment. Additionally, samples might have been mislabeled. Recently, XPS spectra of HAP/urea compounds were revisited but the peak shifts provided were very small.<sup>35</sup> No information on charge calibration was provided; however, if C 1s were used, these peak shifts fall within the error ( $\pm 0.2$  eV) of the calibration method.<sup>48</sup> Finally, a large excess of urea, used to synthesize HAP/urea hybrids, suggests that XPS spectra should contain contributions from both bulk and HAP-bound urea molecules within the vicinity of  $\sim 3$  nm XPS probing layer but no such differences in chemical environments were reported.

In a well-designed experiment, Carmona *et al.* performed the infrared analysis of urea/amorphous calcium phosphate materials and proposed that urea molecules were adsorbed on the surface *via* the interaction of  $\text{NH}_2$  groups, presumably with surface Ca atoms.<sup>23</sup> However, HAP was shown as not necessary to induce a beneficial nitrogen release effect *via* chemical bonding. This effect can be through hydrogen bonds and electrostatic interactions. Silva *et al.* synthesized urea/silica hybrids and examined their chemical binding through FTIR measurements. The experiment showed shifts of vibrational frequencies

attributed to the formation of new hydrogen bonds and other new non-electrostatic forces (physical bonds) through urea amine and carbonyl groups<sup>50</sup> with relatively inert silica. These formed bonds led to sustained-release behavior for more than ten days in water. Silva *et al.* measured and reported by FTIR spectra of HAP/urea where there were  $\sim 19$  and  $14$   $\text{cm}^{-1}$  peaks towards higher wavenumbers for carbonyl stretching ( $\text{C}=\text{O}$ ) and amine bending ( $\text{NH}_2$ ) vibrations, respectively. While agreeing with recent data,<sup>35</sup> this seemingly contradicted previous work where HAP/urea hybrid formation resulted in a peak shift towards lower wavenumbers from pure urea.<sup>34</sup> Similarly, Madusanka *et al.* reported that urea and HAP showed strong interaction which was detected by FTIR. They found that there was an overlap between O–H and N–H vibrations which led to a peak broadening and shifting towards lower wavenumbers.<sup>37</sup> This discrepancy is shown in Fig. 3 and suggests different binding modes based on the synthesis methods.

### 6.3. Theoretical insights *via* density functional theory (DFT)

Fuad *et al.* theoretically investigated the interaction between HAP and urea and reported that urea can be adsorbed and coordinated on the surface of HAP. Using cluster surface approximation and a Gaussian basis set, they showed that the adsorption can take place *via* hydrogen of urea with the oxygen of HAP and carbonyl oxygen of urea with Ca surface atoms of



Fig. 3 Reported FTIR peak shifts of HAP/urea hybrid materials with respect to urea. The results are consistent among 3 researchers, while in contrast with those by Fernando and in most functional groups in Channab's work.<sup>34,35,37,38,49</sup>



HAP.<sup>29</sup> Single (gas) molecule adsorption was used to model the interactions which lack any packing effects since very high loadings of urea are routinely utilized in HAP/urea hybrids. Additionally, HAP is known to possess several very distinct surface terminations (Ca or P rich); hydration and extended solid-state surface simulations are needed to account for those.<sup>51</sup> Recently, Fernando *et al.* studied interactions between urea and HAP and showed that HAP and urea can bind together through several modes but the binding interactions were proposed based on the previous studies of urea–metal complex assignments. They can interact through C=O moieties of urea and  $\text{Ca}^{2+}$  cations, N–H and  $\text{Ca}^{2+}$ , N–H and OH, or N–H and O of  $\text{PO}_4$  which are illustrated in Fig. 4.<sup>35</sup>

Fuad *et al.* calculated the electrostatic potential (ESP) of hydroxyapatite (HAP) and showed that certain regions can be described as electron-rich (negatively charged), while others are electron-deficient (positively charged). The minima points on the potential surface, which are electron-rich, were found near the hydrogen atoms in the OH groups. As a result, these regions are susceptible to electrophilic attack from electron-deficient species (electrophiles). On the other hand, the maxima points were located near the oxygen and calcium atoms, which are relatively electron-deficient. This makes them vulnerable to nucleophilic attack, where electron-rich species (nucleophiles) are attracted to these positively charged areas. The results showed that urea molecules prefer regions on the HAP surface where the charges complement their chemical properties. The nucleophilic atoms in urea (oxygen and nitrogen) moved toward the electrophilic sites (electron-deficient regions), while the electrophilic atoms in urea (hydrogen) were attracted to nucleophilic sites (electron-rich regions) as shown in Fig. 5.<sup>29</sup> Furthermore, the results showed that there is a strong interaction (non-covalent) between oxygen–calcium and hydrogen–oxygen. Another study by Fuad *et al.* showed a new strong bond formed between nitrogen and the nearest calcium atom.<sup>52</sup> These computational studies explain the experiments that noticed the hybrid formation of HAP/urea.



Fig. 5 The non-covalent bonding between HAP and urea through the nucleophile and electrophile sites. Electrophilic sites in urea can be  $-\text{H}$  and  $-\text{Ca}-$  in HAP while nucleophilic sites can be  $-\text{O}-\text{H}$  or  $-\text{N}=\text{O}$  in urea and the hydroxyl group in HAP.

#### 6.4. Nutrient release mechanisms

The bonding between HAP and urea is moderate in strength which consequently reduces the release rate of N and P.<sup>34</sup> Moreover, most of the previous studies showed that the kinetics of HAP/urea hybrid nutrient release follow Higuchi and Korsmeyer–Peppas models that depend on Fickian diffusion, but there also are studies that reported that the diffusion mechanism is non-Fickian.<sup>34,37,38</sup> Indeed, Fickian diffusion behavior provides a rationale for the controlled release of N and P from HAP/urea fertilizers. The elevated concentration of nutrients within the prepared fertilizer instigates a release process directed towards the soil with lower nutrient concentrations (specifically, lower levels of P and N). As the nutrients diffuse into the soil, their concentration increases, leading to a reduction in the release rate until the plants effectively utilize the nutrient elements. Consequently, the soil experiences a decline in the nutrient concentration, allowing the fertilizer to release



Fig. 4 Proposed bonding modes between  $\text{Ca}^{2+}$ ,  $\text{O}_3-\text{PO}_3^-$ , and  $\text{OH}^-$  in HAP with  $-\text{CO}-$  and  $\text{NH}-$  functional groups of urea.<sup>35</sup> Assignments were made based on previous literature reports using metal–urea complexes.



more nutrients gradually. However, Kottegoda *et al.* suggested that urea and HAP/urea had the same mechanism according to the Higuchi model.<sup>34</sup> On the other hand, Maghsoodi *et al.* and Madusankaa *et al.* indicated differences, where urea followed the Higuchi model while incorporating urea in the HAP structure led to following the Korsmeyer–Peppas model.<sup>37,38</sup>

### 6.5. Thermal stability

Thermal stability is a critical factor in understanding the behavior of materials and determining if the material can be suitable for a specific application. Reddi *et al.* performed the characterization of pure urea through differential scanning calorimetry (DSC). They showed a pronounced endothermic peak manifesting around 135 °C.<sup>53</sup> Coordination of urea in hybrid compounds, however, leads to a shift of the peak to higher temperatures. For example, Jeeva *et al.* in their study on urea–hexanedioic acid co-crystals observed that the DSC peak shifted to approximately 150 °C.<sup>54</sup> Exploring polyurethane–urea, Chashmejahanbin *et al.* revealed that DTA registered a peak at around 250 °C for polyurethane–urea, while no corresponding peak was evident in DSC for the melting point of urea until approximately 200 °C.<sup>55</sup> More relevant are recent data from urea inorganic compound cocrystals. In particular, Honer *et al.*

prepared calcium and magnesium salt–urea as cocrystals. They demonstrated that  $\text{Ca}(\text{NO}_3)_2 \cdot 4\text{CO}(\text{NH}_2)_2$  showed an increase in the melting point to 155.5 °C. In addition,  $\text{CaSO}_4 \cdot 4\text{CO}(\text{NH}_2)_2$  increased the melting point to 210 °C.<sup>56</sup> Since co-crystallization affords new bond formation, it changes the fundamental thermal stability of urea and provides a basis for the underlying HAP/urea hybrid thermal stability data analysis.

Sharma *et al.* investigated the impressive thermal stability of HAP which exhibited no degradation even at temperatures as high as 1200 °C. Conversely, urea, a component within the HAP/urea composite, showed significant thermal vulnerability, undergoing complete degradation at a comparatively low temperature of around 350 °C which is much greater than that for pure urea and comparable to that of urea inorganic cocrystals. Notably, the HAP/urea composite exhibited enhanced retention of urea even in a water environment, with 15% of the initial urea content remaining, unreleased within the HAP structure after 100 minutes with a temperature value of around 600 °C.<sup>31</sup> This retention can be attributed to the protective role of HAP, preventing urea's rapid release. Pradhan *et al.* also demonstrated the thermal stability of the HAP/urea composite. Their thermo-gravimetric analysis (TGA) revealed that even after being subjected to temperatures as high as 800 °C, a remarkable 85% of the total mass was preserved.<sup>57</sup> They studied the

Table 4 The detected temperatures by DSC, TGA, and DTA for various urea compounds compared to HAP/urea

Composition	T (°C)	Mass loss or phase change	Technique	Ref.
Pure urea	134	Melting	DSC	58
Pure urea	130–250	Around 70% mass loss	TGA	59
	250–300	Completely decomposed		59
Erythritol	125	Melting	DSC	60
7Erythritol/3urea	120			
Poly(propylene succinate) (PPS)	55	Melting	DSC	58
Poly(butylene succinate) (PBS)	114			
Poly(ethylene succinate) (PES)	103			
Kaolinite	450–525	Approximately 80% mass loss	TGA	59
PPS/urea	137	Melting	DSC	58
PES/urea	140			
PBS/urea	145			
Urea/hexanedioic	150	Melting	DSC	54
	300	Decomposition		
	200–300	All the material has decomposed at 300 °C	TGA	
Carbonaceous material–urea–formaldehyde resin	90	—	DSC	61
Carbonaceous material–urea–formaldehyde resin	150	—		
Polyurethane–urea	200–250	Urea melting	DTA	55
	300–350	—		
	350–450			
Urea–formaldehyde	133	Mass from 100% to 80%	DTA	62
	253	Mass from 80% to 25%		
	310	Mass from 25% to 23%		
Kaolinite–urea by milling	150–250	40% loss	TGA	59
	250–400	Reached 70% loss		
	400–500	90% loss		
Kaolinite–urea by mixing	150–350	60% loss		
	350–500	90% loss		
HAP/urea	25–100 °C	From 100% to around 95 wt%	TGA	43 and 57
	150–200 °C	From 100% to around 75 wt%		
	230–400 °C	From 75% to around 67.5 wt%		



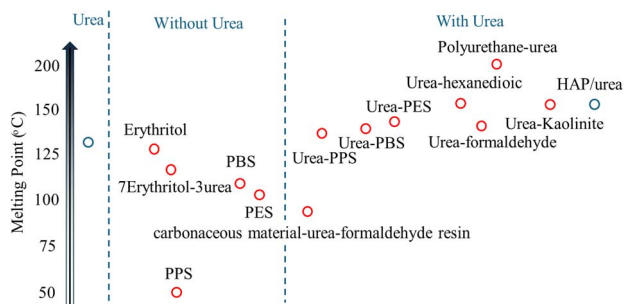


Fig. 6 A graphic representation of the thermal analysis results of parent compounds, reference hybrid materials and co-crystals and HAP/urea. The blue circles indicate urea and HAP/urea, while the red circle indicates the other urea materials including urea cocrystals and urea polymers.

crystallization of HAP crystals with urea addition at different pH values and different aging times. The TGA and DTA results indicated that for HAP crystallization at pH 8, and with no aging time, an endothermic peak occurred around 150–200 °C. Elhassani *et al.* showed TGA of pure urea and the starting point for the first weight loss phase was around 180 °C with a loss of around 60% of its initial weight. On the other hand, HAP/urea maintained 67.5 wt% at around 500 °C which indicated that about 32.5% of urea was left immobilized and bonded with the HAP structure.<sup>43</sup> These results indicate the higher thermal stability of the newly formed structure of HAP/urea compared to the other structures as shown in Table 4.

Hence literature analysis suggests that HAP/urea hybrid materials possess more robust thermal properties than parent urea due to the interactions of the parent compounds. This can be seen in the visual representation based on the onset melting point of the various compounds in Fig. 6.

## 7. Toxicity concerns associated with HAP/urea materials

Nanohydroxyapatite (nHAP) is used in several studies as the basis of the HAP/urea hybrid. It showed significant potential in enhancing plant growth, improving biomass production, and increasing crop yields.<sup>63</sup> This can be expected due to P and Ca nutrients, but nHAP can also enhance the ability of plants to tolerate environmental stress, particularly in soils contaminated with heavy metals.<sup>63–65</sup> When plants are exposed to heavy metal stress, nHAP has been shown to bolster antioxidant enzyme activity which can help plants mitigate the harmful effects of oxidative stress.<sup>63</sup> However, nHAP has toxicity concerns and this is clear when nanoparticles are small enough to penetrate plant cells.<sup>66</sup> Once inside, these particles can interfere with cellular functions, leading to cytotoxic effects that include cell death, reduced plant growth, and lower biomass production. In this regard, Jiang *et al.* found that this toxicity is largely concentration-dependent, meaning that while lower concentrations of nHAP may be beneficial, higher concentrations can have the opposite effect, inhibiting growth and causing harm to the plant. Their experimental results

demonstrated that nHAP inhibited the growth of mung bean sprouts which confirms their cytotoxicity. The smaller nHAP could penetrate cell membranes and enter the cytoplasm, blocking growth. The inhibitory effect depended on the size and concentration of nHAP. At concentrations between 1 and 5 mg mL<sup>-1</sup>, hypocotyl length (HL) decreased from 18 cm to 12 cm as smaller nanoparticles entered the cells. However, at concentrations above 5 mg mL<sup>-1</sup>, the inhibitory effect weakened, with HL increasing to 14 cm due to nanoparticle aggregation and the larger size which prevented further cell penetration.<sup>66</sup> In addition, the sensitivity of plants to nHAP varies among species. Therefore, it is extremely important to study for each species the maximum concentration of nHAP that can be applied to the plant.

## 8. Summary and future perspectives

The utilization of hybrid N–P–(Ca) fertilizer materials composed of HAP and urea has demonstrated significant potential in revolutionizing agricultural practices by offering sustainable and environmentally friendly fertilizers. The incorporation has yielded remarkable outcomes, showing that HAP/urea hybrids can achieve comparable results on plant growth even with reduced nitrogen application rates. This finding is of utmost importance in the context of addressing environmental concerns associated with excessive nitrogen usage in conventional fertilizers. By encapsulating or mixing with urea, the release of nitrogen can be controlled and synchronized with the crop nutrient demands. The studies showed that half or a quarter amount of N is needed for the same results. This controlled-release behavior ensures that plants receive a steady supply of nitrogen over an extended period and reduces nutrient losses through leaching and volatilization. Consequently, the efficient use of nutrients not only improves plant growth but also minimizes the environmental impact caused by nutrient runoff, which contributes to eutrophication and water pollution. The ability of HAP to provide other essential nutrients, such as calcium and phosphorus, is significant besides the nitrogen from urea. Another crucial advantage was the thermal stability, where the HAP/urea melting point increased from that of pure urea and the melting did not complete until approximately 400 °C which shows improvement in overall material stability.

However, the limited number of studies that investigate binding phenomena within the HAP/urea hybrid materials led to a poor understanding of the binding and kinetic characteristics as depicted in Fig. 7. Understanding these binding processes is crucial for optimizing the formulation of HAP/urea hybrids, ensuring their stability and controlled-release properties. These include the binding of carbonyl groups (C=O) in urea with hydroxyl groups in HAP, as well as the interaction between nitrogen–hydrogen (NH) groups in urea and hydroxyl groups in HAP but the data remain incomplete or even controversial. The observed differences appear to be related to the thermal steps of preparation but the available data do not provide conclusive evidence which would lead to the rational design of these materials with tunable properties.





Fig. 7 A summary of the highlighted limitations of HAP/urea hybrid material data available in the literature.

More studies are also needed to establish guidelines and standards for the safe and responsible use of hybrid fertilizers based on HAP nanoparticles. Some studies have shown evidence of toxicity associated with nanomaterials, including HAP nanoparticles smaller than 30 nm.<sup>66</sup> Future perspectives in this field are promising and call for further investigations to unlock the full potential of HAP/urea hybrids. Long-term field trials are necessary to assess the performance of these hybrids under diverse agroclimatic conditions, crop types, and farming practices. Comparative studies between hybrid fertilizers and conventional fertilizers shed light on their economic viability and potential benefits in sustainable agriculture. Moreover, exploring novel compositions based on HAP/urea may lead to the development of even more effective and tailored hybrid formulations. Commercially, the scalability and economic feasibility of HAP/urea hybrids will be significant factors. To facilitate widespread adoption, it is crucial to conduct more research focused on detailed cost estimations and optimization of production methods. For instance, more studies are needed to explore cost-effective and environmentally friendly synthesis techniques, such as ball milling (mechanochemistry) which could help reduce the reliance on more expensive or less sustainable manufacturing processes (cheaper and greener). Investigating and optimizing the efficiency of these hybrids, including nutrient release profiles and performance across diverse soil and climatic conditions, is essential to ensure that these hybrids can be used instead of conventional fertilizers. After enough related research about cost, performance, and toxicity under various conditions, developing a robust supply chain will be a significant step. This stage will be important for reducing production costs while maintaining product quality which means it is cost-effective for farmers. This includes identifying alternative raw materials, reducing energy consumption during production, and streamlining logistics. However, this is a late stage, and the most important stages to focus on currently, are safety, different synthesis methods, and experimenting on various species under several conditions.

## Data availability

No primary research results, software or code have been included and no new data were generated or analysed as part of this review.

## Conflicts of interest

There are no conflicts to declare.

## Acknowledgements

This work was supported by the Engineering for Agricultural Production Systems program grant no. 2020-67022-31144 from the USDA National Institute of Food and Agriculture.

## References

- 1 R. Lal, Feeding 11 billion on 0.5 billion hectare of area under cereal crops, *Food Energy Secur.*, 2016, **5**(4), 239–251.
- 2 J. N. O'Sullivan, Demographic delusions: world population growth is exceeding most projections and jeopardising scenarios for sustainable futures, *World*, 2023, **4**(3), 545–568.
- 3 G. He, X. Liu and Z. Cui, Achieving global food security by focusing on nitrogen efficiency potentials and local production, *Global Food Secur.*, 2021, **29**, 100536.
- 4 S. K. Lam, U. Wille, H.-W. Hu, F. Caruso, K. Mumford, X. Liang, B. Pan, B. Malcolm, U. Roessner and H. Suter, Next-generation enhanced-efficiency fertilizers for sustained food security, *Nat. Food*, 2022, **3**(8), 575–580.
- 5 D. R. Kanter, F. Bartolini, S. Kugelberg, A. Leip, O. Oenema and A. Uwizeye, Nitrogen pollution policy beyond the farm, *Nat. Food*, 2020, **1**(1), 27–32.
- 6 K. Mahmud, D. Panday, A. Mergoum and A. Missaoui, Nitrogen losses and potential mitigation strategies for a sustainable agroecosystem, *Sustainability*, 2021, **13**(4), 2400.
- 7 W. de Vries, Impacts of nitrogen emissions on ecosystems and human health: a mini review, *Curr. Opin. Environ. Sci. Health*, 2021, **21**, 100249.
- 8 D. C. Necula, I. Balta, E. Simiz, M. N. Neagu and L. Stef, Nitrogen emissions from agriculture and livestock sector, among the causes of climate change, *Sci. Pap. Anim. Sci. Biotechnol.*, 2022, **55**(2), 18–23.
- 9 R. Nieder and D. K. Benbi, Reactive nitrogen compounds and their influence on human health: an overview, *Rev. Environ. Health*, 2022, **37**(2), 229–246.
- 10 T. Münzel, O. Hahad, A. Daiber and P. J. Landrigan, Soil and water pollution and human health: what should cardiologists worry about?, *Cardiovasc. Res.*, 2023, **119**(2), 440–449.
- 11 X. Peng, Y. Jiang, Z. Chen, A. I. Osman, M. Farghali, D. W. Rooney and P.-S. Yap, Recycling municipal, agricultural and industrial waste into energy, fertilizers, food and construction materials, and economic feasibility: a review, *Environ. Chem. Lett.*, 2023, **21**(2), 765–801.
- 12 C. E. Nedelciu, K. V. Ragnarsdottir, P. Schlyter and I. Stjernquist, Global phosphorus supply chain dynamics: assessing regional impact to 2050, *Global Food Secur.*, 2020, **26**, 100426.
- 13 A. Rosemarin, B. Macura, J. Carolus, K. Barquet, F. Ek, L. Järnberg, D. Lorick, S. Johannesdottir, S. M. Pedersen and J. Koskiah, Circular nutrient solutions for agriculture



- and wastewater—a review of technologies and practices, *Curr. Opin. Environ. Sustain.*, 2020, **45**, 78–91.
- 14 A. Sharmin, M. A. Hai, M. M. Hossain, M. M. Rahman, M. B. Billah, S. Islam, M. Jakariya and G. C. Smith, Reducing excess phosphorus in agricultural runoff with low-cost, locally available materials to prevent toxic eutrophication in hoar areas of Bangladesh, *Groundw. Sustain. Dev.*, 2020, **10**, 100348.
  - 15 A. K. Tiwari and D. B. Pal, Nutrients contamination and eutrophication in the river ecosystem, in *Ecological Significance of River Ecosystems*, Elsevier, 2022, pp. 203–216.
  - 16 Y. Huang, J. Qian, L. Lu, W. Zhang, S. Wang, W. Wang and X. Cheng, Phosphogypsum as a component of calcium sulfoaluminate cement: hazardous elements immobilization, radioactivity and performances, *J. Clean. Prod.*, 2020, **248**, 119287.
  - 17 A. Es-said, H. Nafai, G. Lamzougui, A. Bouhaouss and R. Bchitou, Comparative adsorption studies of cadmium ions on phosphogypsum and natural clay, *Sci. Afr.*, 2021, **13**, e00960.
  - 18 S. Raguraj, W. Wijayathunga, G. Gunaratne, R. Amali, G. Priyadarshana, C. Sandaruwan, V. Karunaratne, L. Hettiarachchi and N. Kottegoda, Urea-hydroxyapatite nanohybrid as an efficient nutrient source in *Camellia sinensis* (L.) Kuntze (tea), *J. Plant Nutr.*, 2020, **43**(15), 2383–2394.
  - 19 R. Huang, P. Mao, L. Xiong, G. Qin, J. Zhou, J. Zhang, Z. Li and J. Wu, Negatively charged nano-hydroxyapatite can be used as a phosphorus fertilizer to increase the efficacy of wollastonite for soil cadmium immobilization, *J. Hazard Mater.*, 2023, **443**, 130291.
  - 20 S. Tang and X. Fei, Refractory calcium phosphate-derived phosphorus fertilizer based on hydroxyapatite nanoparticles for nutrient delivery, *ACS Appl. Nano Mater.*, 2021, **4**(2), 1364–1376.
  - 21 D. Wang, Y. Jin and D. P. Jaisi, Effect of size-selective retention on the cotransport of hydroxyapatite and goethite nanoparticles in saturated porous media, *Environ. Sci. Technol.*, 2015, **49**(14), 8461–8470.
  - 22 M. Thathsarani, Nanofertilizer for Precision and Sustainable Agriculture, *J. Res. Technol. Eng.*, 2021, **2**(1), 81–85.
  - 23 F. J. Carmona, A. Guagliardi and N. Masciocchi, Nanosized calcium phosphates as novel macronutrient nanofertilizers, *Nanomaterials*, 2022, **12**(15), 2709.
  - 24 M. Usman, M. Farooq, A. Wakeel, A. Nawaz, S. A. Cheema, H. u. Rehman, I. Ashraf and M. Sanaullah, Nanotechnology in agriculture: current status, challenges and future opportunities, *Sci. Total Environ.*, 2020, **721**, 137778.
  - 25 H. Sajadinia, D. Ghazanfari, K. Naghavi, H. Naghavi and B. Tahamipur, A comparison of microwave and ultrasound routes to prepare nano-hydroxyapatite fertilizer improving morphological and physiological properties of maize (*Zea mays* L.), *Heliyon*, 2021, **7**(3), e060941.
  - 26 C. Y. Rao, X. Y. Sun and J. M. Ouyang, Effects of physical properties of nano-sized hydroxyapatite crystals on cellular toxicity in renal epithelial cells, *Mater. Sci. Eng., C*, 2019, **103**, 109807.
  - 27 D. Li, X. Huang, Y. Wu, J. Li, W. Cheng, J. He, H. Tian and Y. Huang, Preparation of pH-responsive mesoporous hydroxyapatite nanoparticles for intracellular controlled release of an anticancer drug, *Biomater. Sci.*, 2016, **4**(2), 272–280.
  - 28 A. Samadi, M. Pourmadadi, F. Yazdian, H. Rashedi and M. Navaei-Nigjeh, Ameliorating quercetin constraints in cancer therapy with pH-responsive agarose-polyvinylpyrrolidone-hydroxyapatite nanocomposite encapsulated in double nanoemulsion, *Int. J. Biol. Macromol.*, 2021, **182**, 11–25.
  - 29 N. A. S. M. Fuad, L. S. Ang, N. N. A. M. Nabil and N. Shuhaime, Theoretical Investigations on the Interactions of Urea with Hydroxyl and Non-Hydroxyl Hydroxyapatite Surface, *Trends Sci.*, 2023, **20**(6), 6558.
  - 30 B. Sharma, M. Shrivastava, L. O. Afonso, U. Soni and D. M. Cahill, Zinc-and magnesium-doped hydroxyapatite nanoparticles modified with urea as smart nitrogen fertilizers, *ACS Appl. Nano Mater.*, 2022, **5**(5), 7288–7299.
  - 31 B. Sharma, L. O. Afonso, M. P. Singh, U. Soni and D. M. Cahill, Zinc- and magnesium-doped hydroxyapatite-urea nanohybrids enhance wheat growth and nitrogen uptake, *Sci. Rep.*, 2022, **12**(1), 19506.
  - 32 M. Ammar, S. Ashraf and J. Baltrusaitis, Nutrient-Doped Hydroxyapatite: structure, Synthesis and Properties, *Ceramics*, 2023, **6**(3), 1799–1825.
  - 33 C. Tarafder, M. Daizy, M. M. Alam, M. R. Ali, M. J. Islam, R. Islam, M. S. Ahommed, M. A. S. Aly and M. Z. H. Khan, Formulation of a Hybrid Nanofertilizer for Slow and Sustainable Release of Micronutrients, *ACS Omega*, 2020, **5**(37), 23960–23966.
  - 34 N. Kottegoda, C. Sandaruwan, G. Priyadarshana, A. Siriwardhana, U. A. Rathnayake, D. M. B. Arachchige, A. R. Kumarasinghe, D. Dahanayake, V. Karunaratne and G. A. Amaratunga, Urea-hydroxyapatite nanohybrids for slow release of nitrogen, *ACS Nano*, 2017, **11**(2), 1214–1221.
  - 35 N. L. Fernando, D. T. Rathnayake, N. Kottegoda, J. S. Jayanetti, V. Karunaratne and D. R. Jayasundara, Mechanistic Insights into Interactions at Urea-Hydroxyapatite Nanoparticle Interface, *Langmuir*, 2021, **37**(22), 6691–6701.
  - 36 R. Ullah, S. Sher, Z. Muhammad, S. A. Jan and M. Nafees, Modulating response of sunflower (*Helianthus annuus*) to induced salinity stress through application of engineered urea functionalized hydroxyapatite nanoparticles, *Microsc. Res. Tech.*, 2022, **85**(1), 244–252.
  - 37 N. Madusanka, C. Sandaruwan, N. Kottegoda, D. Sirisena, I. Munaweera, A. De Alwis, V. Karunaratne and G. A. Amaratunga, Urea-hydroxyapatite-montmorillonite nanohybrid composites as slow release nitrogen compositions, *Appl. Clay Sci.*, 2017, **150**, 303–308.
  - 38 M. R. Maghsoodi, N. Najafi, A. Reyhanitabar and S. Oustan, Hydroxyapatite nanorods, hydrochar, biochar, and zeolite for controlled-release urea fertilizers, *Geoderma*, 2020, **379**, 114644.



- 39 C. Pohshna and D. R. Mailapalli, Engineered Urea-Doped Hydroxyapatite Nanomaterials as Nitrogen and Phosphorus Fertilizers for Rice, *ACS Agric. Sci. Technol.*, 2021, 2(1), 100–112.
- 40 F. J. Carmona, G. Dal Sasso, G. B. Ramírez-Rodríguez, Y. Pii, J. M. Delgado-López, A. Guagliardi and N. Masciocchi, Urea-functionalized amorphous calcium phosphate nanofertilizers: optimizing the synthetic strategy towards environmental sustainability and manufacturing costs, *Sci. Rep.*, 2021, 11(1), 3419.
- 41 O. M. Elshayb, A. M. Nada, K. Y. Farroh, A. A. AL-Huqail, M. Aljabri, N. Binothman and M. F. Seleiman, Utilizing Urea–Chitosan Nanohybrid for Minimizing Synthetic Urea Application and Maximizing *Oryza sativa* L. Productivity and N Uptake, *Agriculture*, 2022, 12(7), 944.
- 42 A. Fihri, C. Len, R. S. Varma and A. Solhy, Hydroxyapatite: a review of syntheses, structure and applications in heterogeneous catalysis, *Coord. Chem. Rev.*, 2017, 347, 48–76.
- 43 C. E. Elhassani, Y. Essamlali, M. Aqlil, A. M. Nzenguet, I. Ganetri and M. Zahouily, Urea-impregnated HAP encapsulated by lignocellulosic biomass-extruded composites: a novel slow-release fertilizer, *Environ. Technol. Innov.*, 2019, 15, 100403.
- 44 L. Abeywardana, M. de Silva, C. Sandaruwan, D. Dahanayake, G. Priyadarshana, S. Chathurika, V. Karunaratne and N. Kottegoda, Zinc-doped hydroxyapatite–urea nanoseed coating as an efficient macro–micro plant nutrient delivery agent, *ACS Agric. Sci. Technol.*, 2021, 1(3), 230–239.
- 45 G. B. Ramírez-Rodríguez, C. Miguel-Rojas, G. S. Montanha, F. J. Carmona, G. Dal Sasso, J. C. Sillero, J. Skov Pedersen, N. Masciocchi, A. Guagliardi and A. Pérez-de-Luque, Reducing nitrogen dosage in *Triticum durum* plants with urea-doped nanofertilizers, *Nanomaterials*, 2020, 10(6), 1043.
- 46 R. Keuleers, H. O. Desseyn, B. Rousseau and C. Van Alsenoy, Vibrational Analysis of Urea, *J. Phys. Chem. A*, 1999, 103(24), 4621–4630.
- 47 H. A. Al-Abadleh and V. H. Grassian, FT-IR Study of Water Adsorption on Aluminum Oxide Surfaces, *Langmuir*, 2003, 19(2), 341–347.
- 48 J. W. Pinder, G. H. Major, D. R. Baer, J. Terry, J. E. Whitten, J. Čechal, J. D. Crossman, A. J. Lizarbe, S. Jafari, C. D. Easton, J. Baltrusaitis, M. A. van Spronsen and M. R. Linford, Avoiding common errors in X-ray photoelectron spectroscopy data collection and analysis, and properly reporting instrument parameters, *Appl. Surf. Sci. Adv.*, 2024, 19, 100534.
- 49 B.-E. Channab, C. E. Elhassani, Y. Essamlali, S. E. Marrane, A. Chakir and M. Zahouily, Urea-loaded hydroxyapatite–carboxylated cellulose composites as slow-release N fertilizer pellets for efficient delivery of nitrogen, *Ind. Eng. Chem. Res.*, 2023, 62(37), 14853–14865.
- 50 M. de Silva, D. P. Siriwardena, C. Sandaruwan, G. Priyadarshana, V. Karunaratne and N. Kottegoda, Urea-silica nanohybrids with potential applications for slow and precise release of nitrogen, *Mater. Lett.*, 2020, 272, 127839.
- 51 D. Kiani and J. Baltrusaitis, Surface chemistry of hydroxyapatite for sustainable n-butanol production from bio-ethanol, *Chem Catal.*, 2021, 1(4), 782–801.
- 52 N. A. S. M. Fuad, L. Ang, N. Shuhaime and M. N. A. Bakar, Simulation of urea–hydroxyapatite by using density functional theory (DFT), *J. Sustainability Sci. Manage.*, 2022, 17(3), 188–197.
- 53 R. S. B. Reddi, S. Ganesamoorthy, P. K. Gupta and R. N. Rai, Phase equilibria, crystallization, thermal and microstructural studies on organic monotectic analog of nonmetal–nonmetal system; urea–4-bromo-2-nitroaniline, *Fluid Phase Equilib.*, 2012, 313, 121–126.
- 54 S. Jeeva, S. Muthu, R. Thomas, B. R. Raajaraman, G. Mani and G. Vinitha, Co-crystals of urea and hexanedioic acid with third-order nonlinear properties: an experimental and theoretical enquiry, *J. Mol. Struct.*, 2020, 1202, 127237.
- 55 M. R. Chashmejahanbin, H. Daemi, M. Barikani and A. Salimi, Noteworthy impacts of polyurethane-urea ionomers as the efficient polar coatings on adhesion strength of plasma treated polypropylene, *Appl. Surf. Sci.*, 2014, 317, 688–695.
- 56 K. Honer, E. Kalfaoglu, C. Pico, J. McCann and J. Baltrusaitis, Mechano-synthesis of Magnesium and Calcium Salt–Urea Ionic Cocrystal Fertilizer Materials for Improved Nitrogen Management, *ACS Sustain. Chem. Eng.*, 2017, 5(10), 8546–8550.
- 57 S. Pradhan, M. Durgam and D. R. Mailapalli, Urea loaded hydroxyapatite nanocarrier for efficient delivery of plant nutrients in rice, *Arch. Agron. Soil Sci.*, 2021, 67(3), 371–382.
- 58 H.-M. Ye, H.-F. Li, C.-S. Wang, J. Yang, G. Huang, X. Meng and Q. Zhou, Degradable polyester/urea inclusion complex applied as a facile and environment-friendly strategy for slow-release fertilizer: performance and mechanism, *Chem. Eng. J.*, 2020, 381, 122704.
- 59 S. Seifi, M. T. Diatta-Dieme, P. Blanchart, G. L. Lecomte-Nana, D. Kobor and S. Petit, Kaolin intercalated by urea. Ceramic applications, *Constr. Build. Mater.*, 2016, 113, 579–585.
- 60 N. Feng, Z. Kang and D. Hu, Shape-stabilized and antibacterial composite phase change materials based on wood-based cellulose micro-framework, erythritol-urea or erythritol-thiourea for thermal energy storage, *Sol. Energy*, 2021, 223, 19–32.
- 61 T. A. Khan, A. Gupta, S. S. Jamari, M. Nasir, S. Jang, H.-J. Kim and M. Asim, Synthesis of micro carbonaceous material by pyrolysis of rubber wood and its effect on properties of urea-formaldehyde (UF) resin, *Int. J. Adhes. Adhes.*, 2020, 99, 102589.
- 62 M. Biswas and S. Bandyopadhyay, Nano-crystalline Pr<sup>3+</sup>-ceria powder by urea–formaldehyde gel combustion route, *Adv. Powder Technol.*, 2014, 25(2), 536–542.
- 63 M. R. Maghsoodi, L. Ghodszad and B. A. Lajayer, Dilemma of hydroxyapatite nanoparticles as phosphorus fertilizer: potentials, challenges and effects on plants, *Environ. Technol. Innov.*, 2020, 19, 100869.
- 64 L. Yang, B. Liu, Y. Lu, F. Lu, X. Wu, W. You and B. Huang, Bioavailability of cadmium to celery (*Apium graveolens* L.)



## Critical Review

- grown in acidic and Cd-contaminated greenhouse soil as affected by the application of hydroxyapatite with different particle sizes, *Chemosphere*, 2020, **240**, 124916.
- 65 X. Zeng, H. Xu, J. Lu, Q. Chen, W. Li, J. Tang and L. Ma, The immobilization of soil cadmium by the combined amendment of bacteria and hydroxyapatite, *Sci. Rep.*, 2020, **10**, 2189.
- 66 H. Jiang, J.-K. Liu, J.-D. Wang, Y. Lu, M. Zhang, X.-H. Yang and D.-J. Hong, The biotoxicity of hydroxyapatite nanoparticles to the plant growth, *J. Hazard. Mater.*, 2014, **270**, 71–81.

